Colloids and Surfaces B: Biointerfaces 190 (2020) 110894

Contents lists available at ScienceDirect

Colloids and Surfaces B: Biointerfaces

journal homepage: www.elsevier.com/locate/colsurfb

A comparative analysis of detachment forces and energies in initial and mature cell-material interaction

Philipp Wysotzki[a,1], Ana Sancho[b,c,1], Jan Gimsa[a,2,*], Jürgen Groll[b,2]

[a] Department of Biophysics, Faculty of Natural Sciences, University of Rostock, Gertrudenstr. 11a, 18057 Rostock, Germany
[b] Department of Functional Materials in Medicine and Dentistry and Bavarian Polymer Institute (BPI), University of Würzburg, Pleicherwall 2, 97070 Würzburg, Germany
[c] Department of Automatic Control and Systems Engineering, University of the Basque Country UPV/EHU, Plaza de Europa 1, 20018 Donostia, Spain

ARTICLE INFO

Keywords:
Cell adhesion
Single cell force spectroscopy
Single cell force microscopy
FluidFM
MC3T3 osteoblast-like cells
L929 fibroblast cells
Protein coatings
Collagen
Fibronectin

ABSTRACT

Single cell force spectroscopy (SCFS) enables data on interaction forces to be acquired during the very early adhesion phase. However, SCFS detachment forces and energies have not been compared so far with the forces and energies after maturation of the cell-material contact on a single cell level and with comparable time resolution. We used FluidFM® to physically attach single cells to the cantilever by aspiration through a microfluidic channel, in order to achieve the higher forces required for detaching maturely adhering cells. Combining these two approaches allowed us to compare cell adhesion in the initial and maturation phases of adhesion for two exemplary cell-substrate combinations – L929 fibroblasts on fibronectin and MC3T3 osteoblasts on collagen type I. Uncoated glass substrates were used as a reference. For both cell lines, SCFS measurements after contact times of 5, 15 and 30 s revealed significantly higher maximum detachment forces (MDFs) and energies on glass compared to the protein-coated surfaces in the 0.5–4 nN (1–40 fJ) range. FluidFM® measurements after 1, 2 and 3 days of culture revealed a significant absolute increase in the MDFs and detachment energies for both cell lines on protein-coated substrates to values of about 600 nN and 10 pJ. On glass, the MDFs were similar for MC3T3 cells, while they were significantly lower for L929 cells. For both cell types, the differences in detachment energy were significant. These differences underline the importance of investigating early and mature adhesion states to obtain a holistic assessment of the cell-material interactions.

1. Introduction

Modern biomaterials research focuses on the development and design of materials that actively interact with the surrounding cells, with the final aim of obtaining tissue regeneration. Consequently, culture materials and scaffolds that favor cell adhesion and proliferation are usually investigated [1,2] and which ideally allow specific and biomimetic cell adhesion mechanisms to occur [3–5]. The proper understanding of cellular adhesion onto materials is crucial in identifying design criteria for biomaterials research.

Cell adhesion onto substrates is a dynamic process consisting of different phases. Nonadherent cells are usually round. Their initial attachment is governed by electrostatic interaction with the substrate, during which single molecules start to adhere. As more and more molecules adhere, the cells begin to flatten and integrins start binding to the substrate's surface. Finally, these transitory stages lead to a full spreading of the cells and maturation of the focal adhesions contacts, characteristic for the steady adhesion state of cultured cells [6,7]. Although initial cell adhesion is fast, processes such as the aggregation of vinculin and cadherins, which form part of the cytoskeleton remodeling, only take place about 100 s after force induction [8]. More mature focal adhesion complexes take several minutes to establish [9], although recent studies have shown that certain integrins respond to stress in less than a second [10]. The first 5 – 20 min of adhesion are therefore generally considered as the "initial adhesion" phase.

Adhesion forces of cells to substrates can be studied using a variety of techniques, such as flow chambers or spinning disks [11,12]. The spinning disk assay was developed for a better control of the applied detachment forces. It permits the application of defined shear forces to the cells on a surface by varying the rotational speed of the disk [13]. Nevertheless, in the spinning disk assay, the mechanical detachment of cells not only depends on the strength, number and distribution of the

* Corresponding author.
E-mail address: jan.gimsa@uni-rostock.de (J. Gimsa).
[1] Equally contributing first authors.
[2] Equally contributing corresponding authors.

https://doi.org/10.1016/j.colsurfb.2020.110894
Received 30 October 2019; Received in revised form 14 January 2020; Accepted 20 February 2020
Available online 21 February 2020

adhesion-mediating surface proteins but also on the contact surface and geometry of the individual cells. Therefore, the technique lacks precision in measuring the detachment force of individual cells. The highly sensitive atomic force microscopy (AFM) was used for developing new scanning probe techniques, e.g. with single cells as probes on special cantilevers. This is the setup of the single cell force spectroscopy (SCFS), which is the preferred tool for assessing individual cell adhesion forces. However, the complementary precise measurement of the high adhesion forces after longer periods of cell adhesion has, for a long time, imposed a challenge [14]. The measurement of cell adhesion forces after maturation of focal adhesions was restricted to the maximum immobilization force between a cell and the measuring AFM probe, increased by the chemical functionalization of the cantilever [14,15]. Technological advances have overcome this limitation by replacing the conventional AFM cantilever with a hollow cantilever connected to a pumping system, which permits much higher forces to be exerted onto single cells [16,17]. Originally, this single cell technique called FluidFM® (abbreviated in this paper as FFS – fluidic force spectroscopy) had been used for microinjecting dyes into individual living cells and even into selected subcellular structures [17]. Potthoff et al. [16] were the first to show that the very high immobilization forces between the cantilever and a cell applied by the pump system could be used to overcome the cell adhesion forces even after the complete maturation of the focal contacts, which are representative of the real culture conditions. These authors showed that the setup can be used to measure the maximum detachment forces (MDFs) of strongly adherent cells [16,18,19]. We have advanced this approach and demonstrated that cells can even become detached out of confluent monolayers, resulting in MDFs which, when compared to the values for single adherent cells, give access to values of intercellular adhesion forces [19].

In this study, we have combined the traditional SCFS technique with that of the FFS in order to compare the effects of non-specifically modified surfaces and surfaces with specific adhesion-promoting proteins on the development of cell adhesion forces and energies, from the early initial phase of adhesion to the mature adhesion phase. To investigate cell type and substrate-specific behavior, we chose the L929 mouse fibroblasts cell line and MC3T3 osteoblast-like cells as model systems for measuring their MDFs and detachment energies to standard surfaces coated with fibronectin (L929) or collagen type I (MC3T3) under their established culture conditions. The L929 standard cell line was used because these cells are able to specifically bind fibronectin and are often used for biocompatibility testing [20,21]. The MC3T3 cell line was chosen as the second model system because these cells can specifically interact with collagen, which plays an important role in cartilage and bone formation, via membrane-bound proteins [22–24]. Glass substrates were used as unspecific control surfaces for both [25]. Our results show significant differences in the behavior of the two model systems. In the initial adhesion phase, when electrostatic forces dominate, higher detachment forces and energies on non-specific surfaces were observed in the two cell lines than on protein-coated surfaces [6,7,26]. This tendency was inverted in the later adhesion stages, when focal adhesion forces dominated and the stronger detachment forces and energies on protein-coated surfaces were measured.

2. Materials and methods

2.1. Cell culture

L929 fibroblasts and osteoblast-like MC3T3 cells were obtained from the German collection of microorganisms and cell culture (DSMZ, Braunschweig, Germany). The L929 cells were cultured in Dulbecco's Modified Eagle's Medium (DMEM, order No. F 0415). For the MC3T3 cells, alpha MEM (ord. No. F 0925) was used. Both media were supplemented with 1 % penicillin/streptomycin, 1 % L-glutamine and 10 % fetal bovine serum (all purchased from Biochrom AG, Berlin, Germany).

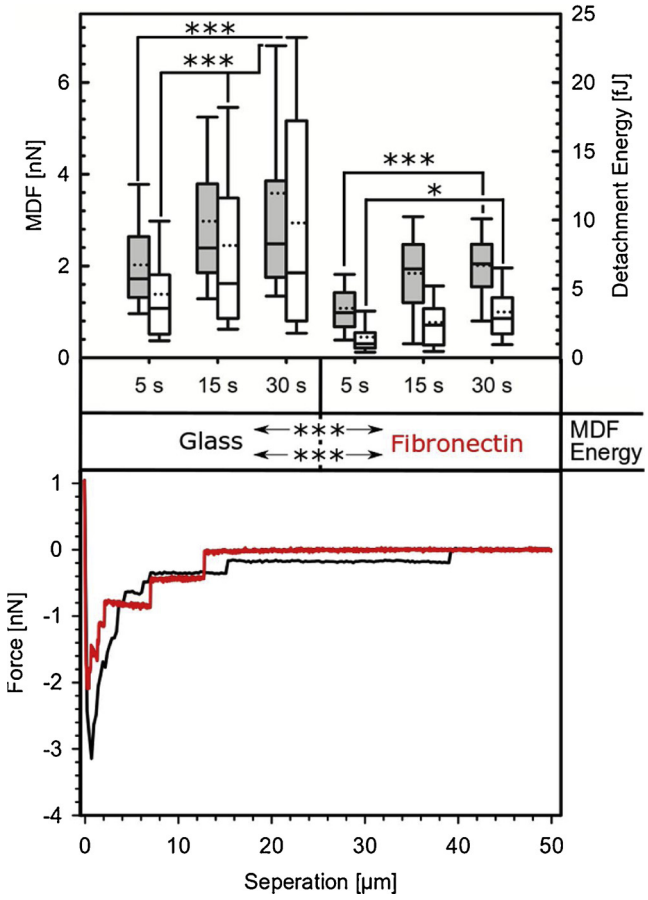

Fig. 1. SCFS of L929 cells on glass and fibronectin. Top: Gray and white boxes indicate MDFs and detachment energies. Significant differences in the MDFs and detachment energies between the different contact times are marked by asterisks. The dotted and solid lines represent the mean values and medians, respectively. Center: Two-way ANOVA comparison of the glass and fibronectin groups revealed statistically significant differences (asterisks) for the MDFs and detachment energies. Bottom: Representative retract force-distance curves after 30-s contact time on glass (black curve) and fibronectin (red curve) surfaces. Number of sampled cells: 8. (For interpretation of the references to colour in the Figure, the reader is referred to the web version of this article).

The incubator ensured 95 % humidity in a 5 % CO_2 atmosphere at a temperature of 37 °C. For the FFS experiments, the cells were trypsinated and transferred to the different measuring surfaces. The cells had been detached with Accutase (PAN-Biotech GmbH, Aidenbach, Germany) and suspended in PBS before the SCFS experiments.

2.2. Surface preparation

2.2.1. Fibronectin

Human plasma fibronectin (Millipore, Cat. No. FC010 – 5 mg) was diluted to 25 µg/ml in PBS. For FFS experiments cover slips of 12 mm in diameter (Gerhard Menzel GmbH, Braunschweig, Germany) were placed in an untreated 24-well plate, before 300 µl of the diluted fibronectin solution was added to each well and incubated at 37 °C for 1 h. The fibronectin coating was freshly prepared before every experiment. Later, in a final stage, the cover slips were rinsed thoroughly with PBS and with culture medium. The protocol differed slightly for the SCFS measurements. Here, 32-mm round cover slips (Gerhard Menzel GmbH, Braunschweig, Germany) were only partially coated by applying droplets of 10 – 15 µl of the solution, before they were treated as described above.

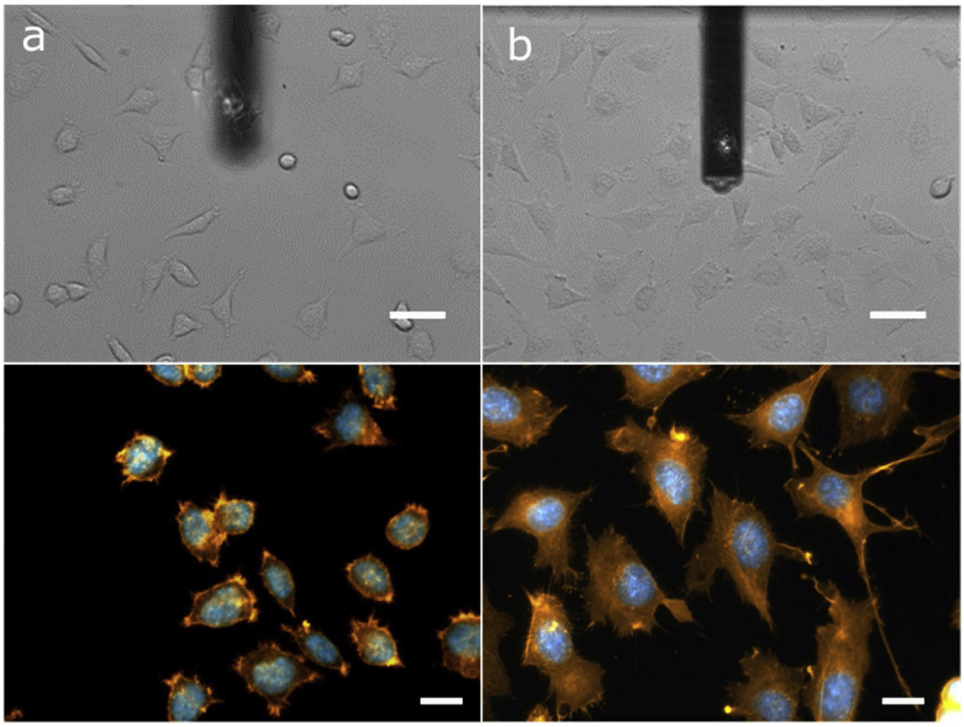

Fig. 2. Bright-field (top; scale bar 50 µm) and fluorescence images (bottom, scale bar 20 µm) of L929 on glass (a) and fibronectin coating (b) one day after cell seeding (DIV 1). FFS cantilever before (top, a) and after approach (top, b). Bottom: F-actin of the cytoskeleton is visualized by phalloidin staining (orange). Cell nuclei are stained with DAPI (blue). (For interpretation of the references to colour in the Figure, the reader is referred to the web version of this article).

2.2.2. Collagen

In order to coat the surfaces with fibrillar collagen Type I, the manufacturer's protocol was followed. In short, the stock solution of collagen A at 1 mg/ml (0.1 % in HCl, Biochrom AG, Berlin, Germany) was diluted with the same volume of 0.3 M NaCl solution, resulting in a final concentration of 0.5 mg/ml. The pH was adjusted to between 7.0 and 8.0 with 1 N NaOH. For the SCFS measurements, a round, the 32-mm glass cover slip was partially coated with a drop of 10–15 µl of the solution. For the FFS measurement, however, the entire surface was covered with the solution. Both were then dried overnight at room temperature in the air flow of a laminar air flow box and stored at 4 °C. Before use, the surfaces were briefly rinsed with PBS or culture medium.

2.3. Single cell force measurements

2.3.1. Initial cell adhesion - SCFS

The cover slip, coated with either collagen or fibronectin, was placed in the Petri dish heater (PetriDishHeater™, JPK, Berlin, Germany) and transferred to the microscope stage of an Axio Observer A1 microscope (Zeiss, Oberkochen, Germany), which was part of the SCFS setup. The Petri dish was filled with 3 ml PBS and heated to 37 °C. For measuring purposes, a cantilever (Arrow TL-1, Nanoworld, Neuchatel, Switzerland) was functionalized with poly-dopamine. The cantilever was cleaned using UV-ozone with UV-C fluorescent tubes (2 × 8 W, Dinies Technologies GmbH, Villingendorf, Germany) for 180 s to remove all types of contamination. It was then later carefully submerged in a 100 µl droplet of PBS-buffer. Then, a 2-µl volume of a freshly prepared dopamine hydrochloride (Sigma Aldrich, St. Louis, USA) solution (5 mg/ml DOPA − HCl in 5 % acetic acid) was added.

Poly-dopamine is highly adhesive and has been shown to be capable of robustly immobilizing a large number of biomolecules on a variety of surfaces [27,28]. It is generally accepted that the catechol group and the amino group play a crucial role in the adhesive properties, although the exact mechanism of adhesion is still unclear [29–31]. The formation of poly-dopamine was induced by a pH shift to alkaline condition, by adding 2 µl sodium hydroxide (2 M). The solution was incubated at room temperature for 25 min and washed with a large amount of PBS afterwards. The cantilevers were mounted on the AFM stage (CellHesion/Nanowizard II AFM, JPK Instruments, Berlin, Germany), then placed on the microscope stage and submerged in the Petri dish filled with PBS. The cantilever was calibrated above a non-coated area by the thermal noise method, using the second harmonic frequency [32]. In order to attach a cell to the cantilever, 100 µl of suspended cells was introduced into the Petri dish; the cantilever was then aligned over a sedimented single cell and approached carefully. The cantilever was pressed onto the cell with a force of 2–6 nN for approx. 30 s before the cantilever was fully retracted. It was left to rest in this position for 10 min in order to ensure a firm contact between the cell and the cantilever.

For SCFS measurements, the retraction and approach velocities were set to 5 µm/s. The cells were approached until a setpoint force of 1 nN was reached. Before retraction, the force was kept constant for 5, 15 and 30 s, respectively. At least 20 force-distance curves were captured for each condition. A fresh cantilever was used for every cell measured for SCFS.

2.3.2. Mature cell adhesion – FFS

L929 and MC3T3 cells were seeded on the uncoated and coated glasses at densities between 20.000 and 35.000 cell/cm^2. At these densities, the cells are not confluent and remain without any contact to neighboring cells for up to three days. Consequently, the MDFs measured refer only to the interaction with the substrate [19]. Cell adhesion forces at the late state were measured using a Flex-FPM system (Nanosurf GmbH, Langen, Germany) combined with the FFS technique (FluidFM®, Cytosurge AG, Glattbrugg, Switzerland). The system was mounted on an Axio Observer Z1 inverted microscope (Carl Zeiss, Oberkochen, Germany) and a piezoelectric stage with a 100-µm retraction range. Use was made of 200 µm long and 36-µm wide Micropipette cantilevers of 8-µm diameter aperture and 2-N/m nominal spring constant (Cytosurge AG, Glattbrugg, Switzerland). The cantilevers were approached at 5 µm/s until a set point of 50 nN was reached. Under constant force, a pause of 3 s followed, where -800 mbar of suctioning pressure was applied to immobilize the cell at the aperture of the cantilever. The stage was then withdrawn at a velocity of 5 µm/s to between 30 µm and 95 µm and the suction pressure maintained until

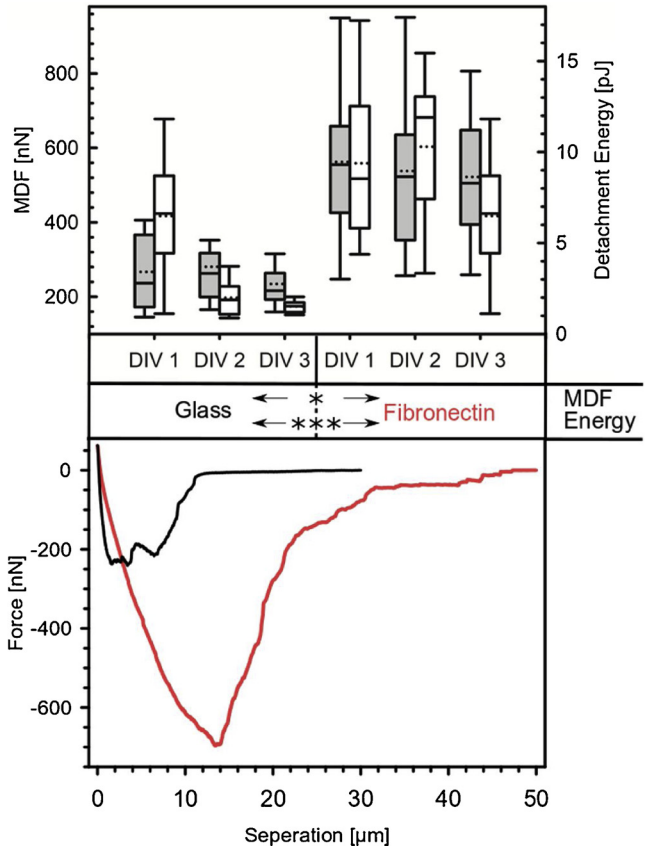

Fig. 3. FFS of L929 cells on glass and fibronectin after complete spreading and maturation of focal adhesions at 1, 2 and 3 days in vitro (DIV). Top: Gray and white boxes indicate MDFs and detachment energies, respectively. Center: Differences between glass and fibronectin-coated substrates are statistically significant for all three time-points ($p < 0.05$, not marked). Bottom: Representative retract force-distance curves on fibronectin-coated (red) and uncoated glass (black) at DIV 3. Number of sampled cells ≥ 20. (For interpretation of the references to colour in the Figure, the reader is referred to the web version of this article).

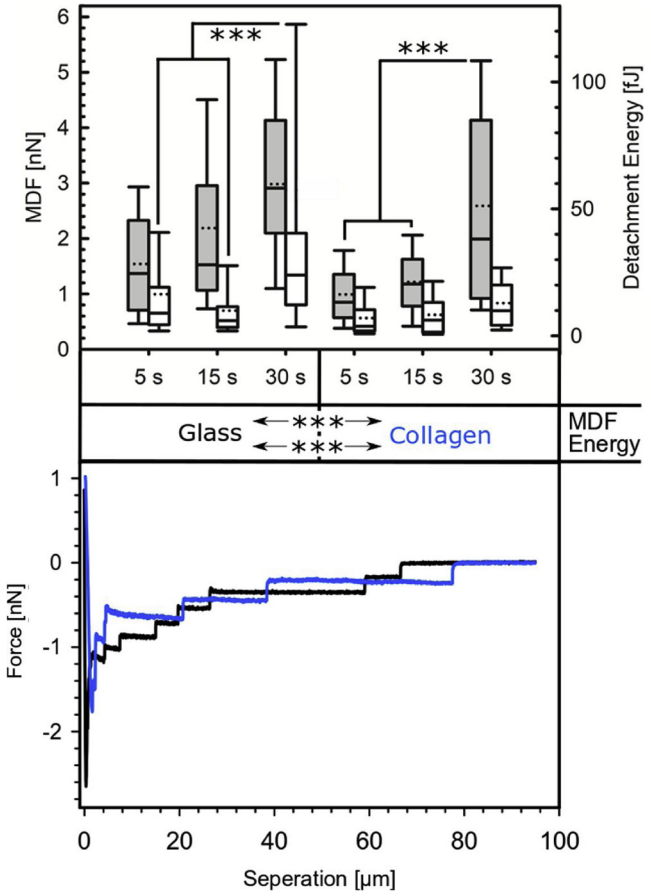

Fig. 4. SCFS of MC3T3 cells on glass and collagen. Top: Gray and white boxes indicate MDFs and detachment energies. Significant differences in the MDFs and detachment energies between the different contact times are marked by asterisks. Center: Two-way ANOVA comparison of the glass and collagen groups revealed highly significant differences for the MDFs and detachment energies (asterisks). Bottom: Representative retract force-distance curves after 30-s contact time on glass (black curve) and collagen (blue curve) surfaces. Number of sampled cells 7. (For interpretation of the references to colour in the Figure, the reader is referred to the web version of this article).

the cell was completely detached from the substrate.

2.3.3. Analysis of the force-distance curves

The maximum peak of the force-distance curve of retraction indicated the MDF, a common indicator of the adhesion forces of the cells. The adhesion energy is usually associated with the detachment energy obtained by integrating the force-distance curve. We used the JPKSPM Data Processing software (JPK Instruments, Berlin, Germany) for analyzing the SCFS force-distance curves. The FFS data were captured using the Cytosurge software (Cytosurge AG, Glattbrugg, Switzerland) and analyzed with SPIP 6.2.0 (Image Metrology, Lyngby, Denkmark) for automatic MDF detection. To calculate the adhesion energies, the force-distance curves were integrated with a self-written SciLab (ESI group, Orsay Cedex, France) script. Prior to integration, the JPKSPM Data Processing software (JPK Instruments, Berlin, Germany) as well as our script corrected the zero force at sufficient separation distances, as well as the tilt caused by thermal drift. Statistical evaluations of MDFs and detachment energies were performed with two-way ANOVA (post hoc Student-Newman-Keuls Method) using Sigmaplot software (Systat Software, Erkrath, Germany). In the diagrams, the significance levels are marked with "*" and "***" for $p < 0.05$ and $p < 0.001$.

2.4. Fluorescence microscopy

Cells seeded on cover slips were first fixed with 4% formalin for 15 min. After thorough washing with PBS they were permeabilized with Triton-X100 diluted to 0.05 % in PBS by incubating the cells in this solution for 15 min. After thorough washing with PBS, samples were incubated with AlexaFluor 555-conjugated Phalloidin (Thermo Fisher Scientific, Waltham, MA, USA) in order to visualize F-actin, while cell nuclei were counterstained with DAPI (4′,6-Diamidin-2-phenylindol, Invitrogen, Carlsbad, CA, USA). Images were taken with an Axio Observer Z1 inverted microscope (Carl Zeiss, Oberkochen, Germany).

3. Results and discussion

3.1. L929 cells on fibronectin

MDFs of L929 mouse fibroblasts from glass surfaces coated with fibronectin as adhesion-promoting specific protein were compared with MDFs from uncoated glass surfaces. Fig. 1 summarizes the results of the SCFS measurements (A L929 cell on a SCFS cantilever is shown in Bright field (top; scale bar 50 µm) and fluorescence images (bottom, scale bar 20 µm) of MC3T3 cells on glass S1 of the supplementary materials).

As expected, the MDFs were higher for longer contact times on fibronectin-coated and uncoated glass, even though the MDF differences between the 15-s and 30-s contact times were insignificant. On the uncoated glass, the standard deviation increased up to the 30-s contact

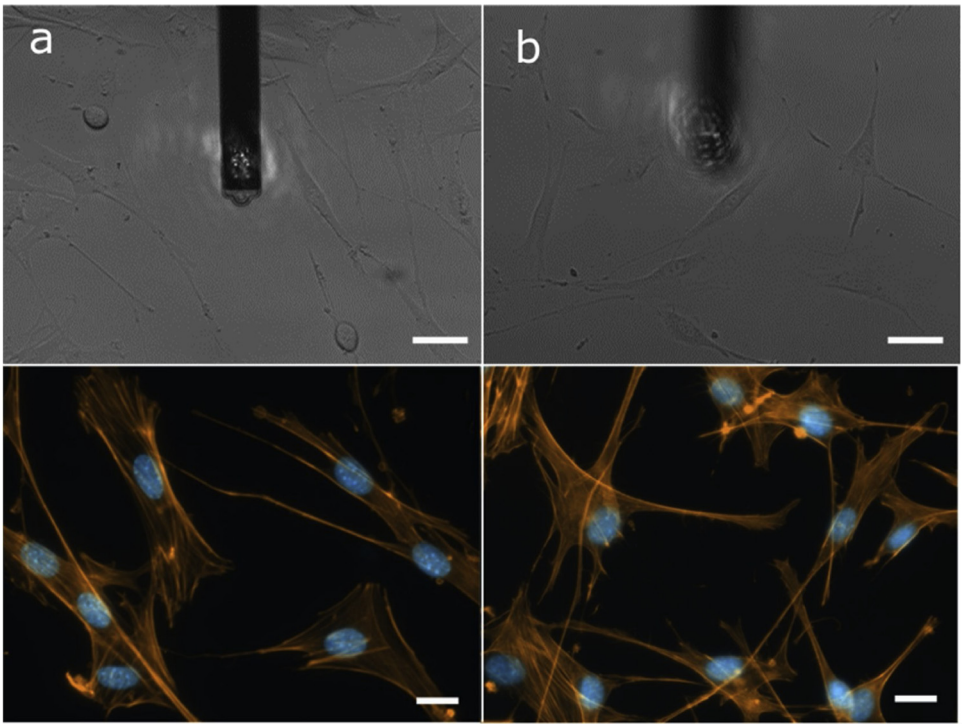

Fig. 5. Bright field (top; scale bar 50 µm) and fluorescence images (bottom, scale bar 20 µm) of MC3T3 cells on glass (a) and collagen coating (b) one day after cell seeding (DIV 1). FFS cantilevers before (top, b) and after approach (top, a). Bottom: F-actin of the cytoskeleton is visualized by phalloidin staining (orange). Cell nuclei are stained with DAPI (blue). (For interpretation of the references to colour in the Figure, the reader is referred to the web version of this article).

time. On fibronectin, the standard deviation at a 30-s contact time was lower than at the 15-s contact time, indicating the onset of stabilization of cell-surface contact. The MDFs were significantly higher for uncoated glass than on the fibronectin-coated surface. This difference is consistent with the view that cell-surface interaction in the first phase of cell adhesion is predominantly driven by electrostatic forces. The stronger, more specific adhesion mechanisms controlled by molecular lock-and-key interactions call for a precise alignment and localization of fibronectin lasting more than 10 min with adhesion-promoting membrane proteins [6]. In particular, the upregulation of specific genes and the synthesis of proteins takes much longer than 30 s [33].

After 24 h in culture (DIV 1) the cells were fully spread, all the transition phases were completed and stable adhesion was achieved (Fig. 2). For *in vitro* contexts, this is the most representative case. MDFs and detachment energies were measured with FFS 24 (DIV 1), 48 (DIV 2) and 72 h (DIV 3) after cell seeding (Fig. 3). After this time, the cells were more strongly bound to the fibronectin-coated substrate than to the uncoated glass, suggesting stronger binding forces through specific, rather than non-specific adhesion mechanisms. Apparently, these specific bonds lead to a reversal of the force relationships between the coated and uncoated substrate in the initial adhesive phase. The MDFs of both surfaces were not significantly different for DIV 1–3 (Fig. 3). This indicated that the cells had already reached their stable regime of adhesion at DIV 1. The standard deviation was considerably lower on glass than on fibronectin, which could be attributed to the heterogeneities of the fibronectin coating at the micro scale. For fibronectin, the areas under the force-distance curves and the corresponding detachment energies were larger. The curves show a series of detachment events that differ between cells and which could be related to the detachment of focal contacts (Fig. 3). According to our current knowledge, it cannot be excluded that some events may be caused e.g. by the rupture of intracellular structures, the rupture of the cell membrane or the deformation of intracellular structures due to the strain caused by the high negative pressure in the microchannel of the cantilever [34,35].

Fluorescence imaging of the actin cytoskeleton on DIV 1 showed that cells cultured on fibronectin were flatter and had a larger spreading area; they differed in cytoskeleton compared to cells cultured on glass, while the size of their nuclei remained unchanged (Fig. 2). These differences correspond to a L929 cell distribution, which is influenced by the presence and density of the fibronectin layer [36]. Phalloidin, which stains the filaments and bundles of the actin cytoskeleton, also shows that cells cultured on fibronectin have increased the formation of actin filaments, which have increased adhesion. Overall, these differences in the actin cytoskeleton, together with the increased spreading area of the cells, caused the higher MDFs measured with FFS on the fibronectin-coated surfaces.

3.2. MC3T3 cells on collagen

MC3T3 cells on collagen-coated surfaces were used as a second cell-surface pair. Glass cover slips coated with fibrillar collagen type I films are soft polymeric substrates with a modulus of elasticity of approx. 5 kPa (cf. supplementary material). As already observed with L929 cells, SCFS measurements on MC3T3 cells revealed MDFs that were higher on the uncoated glass than on coated surfaces for the same contact times (Fig. 4). The MDFs measured were of the same order of magnitude as with the L929 cells.

Similar to L929 cells, MC3T3 cells on glass show increasing MDFs for longer contact times. In contrast to L929 cells on fibronectin, the standard deviation of MDFs for MC3T3 cells on collagen did not decrease over longer contact times, indicating a less stable interaction.

At DIV 1, the MC3T3 cells had been fully spread out. Their shape was largely identical on both surfaces (Fig. 5). This was confirmed by fluorescence imaging, which showed that the stress fibers of the actin cytoskeleton on glass and collagen were very similar. In contrast to fibronectin, where the cell spread area increased and more abundant actin filaments were observed compared to the uncoated surface, cells seeded on collagen revealed no differences in either the spread or the organization of the actin cytoskeleton (cf. Figs. 2 and 5).

FFS measurements showed MDFs that were more than 100 times higher than those measured with SCFS. The differences between the uncoated and coated surfaces of the MDFs observed in the first adhesion phases were altered (Fig. 6). Only two time points, one and two days after cell seeding, were tested with FFS in the mature phase of adhesion. Due to their rapid proliferation, the cells had already established direct

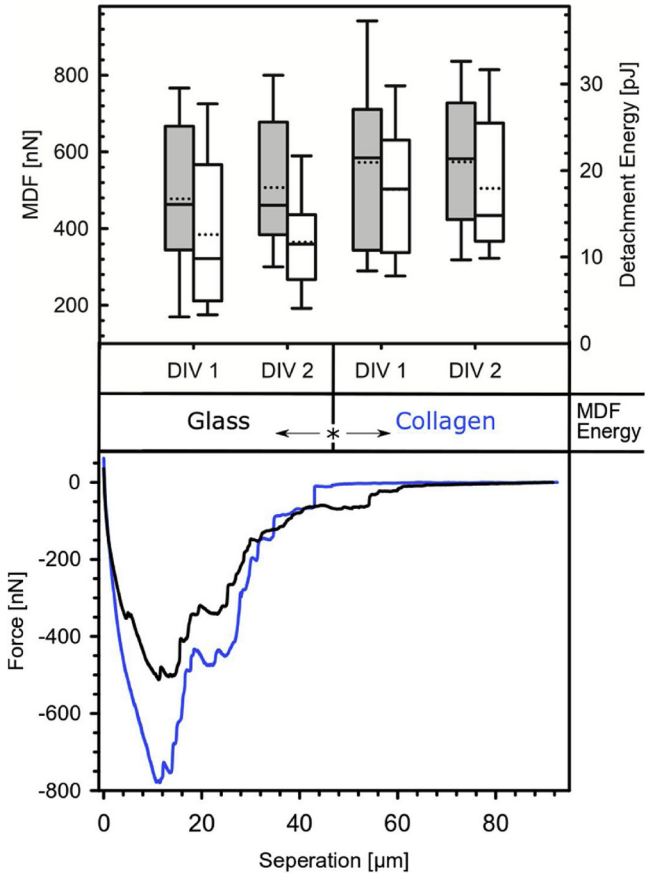

Fig. 6. FFS of MC3T3 cells on glass and collagen after complete spreading and maturation of focal adhesions at 1 and 2 DIV. Top: Grey and white boxes indicate MDFs and detachment energies. Center: A statically significant difference between glass and collagen was observed only in the detachment energies. Bottom: Representative retract force-distance curves on collagen-coated (blue) and uncoated glass (black) at DIV 2. Number of sampled cells ≥ 20. (For interpretation of the references to colour in the Figure, the reader is referred to the web version of this article).

mutual contacts on the third day, even if they had been seeded with a very low cell density. Measurements beyond the second day were not considered in order to focus on the forces between the cells and the substrate and to exclude any contributions from intercellular interaction forces [19].

In the late adhesion phase, collagen MDFs were slightly higher than glass MDFs with no significant differences between the two groups. Nevertheless, significant differences were found in the corresponding detachment energies. Moreover, the force-distance curves of MC3T3 cells showed more detachment events than with L929 cells. This might be related to the spread cell shape with long distributed protrusions and a corresponding distribution of the focal adhesion points.

It is known that MC3T3 cells are able to secrete collagen and thus remodel the surface on which they grow [37–39]. The low stiffnesses of 5300 Pa at DIV1 and 5600 Pa at DIV2 for the collagen coating results shown in the supplementary material, may have prevented a more significant increase in adhesion forces since it is known that cells detect substrate stiffness and microstructure and react accordingly [40–42]. More precisely, cells grown on soft matrices show reduced spread and less stable focal adhesions, which directly influence cell adhesion forces [43–45]. These findings are consistent with the insignificant MDF differences between the two surfaces. However, our results are not sufficient to analyze the effects of substrate stiffness on MDFs and detachment energies.

3.3. Initial and mature adhesion

Taken together, the combined results of SCFS and FFS showed a difference of two orders of magnitude in relation to the adhesion forces that cells exert on the substrate, when comparing their initial and mature phases of adhesion. While the MC3T3 and L929 cells adhered more strongly to the uncoated substrates in the early phase, they did tend to adhere more strongly to substrates coated with their specific adhesion protein in the mature phases of adhesion. These variations were due to the different adhesion mechanisms. While electrostatic interactions and membrane tension [46] are the dominant counteracting factors in the early phase of initial adhesion, adhesion in the mature phase, when cell spreading is complete, is mainly determined by the properties of the focal adhesion complexes [47–49]. It is generally accepted that positively charged substrates promote the adhesion of the negatively charged cell surfaces. Accordingly, it could be assumed that glass surfaces, which are negatively charged, would electrostatically retard cell adhesion. However, Hoshiba et al. were able to show that cells in a serum-free environment adhere evenly good to both negatively and positively charged polymer surfaces within less than 30 min [50].

Our FFS results are in line with the view that specific adhesion proteins are the main determinant for the strong adhesion in the mature phase. It must be mentioned that we performed - in contrast to the FFS experiments - the SCFS experiments in PBS, which was largely lacking Mg^{2+} ions. Because the activation of certain integrins is magnesium-dependent [51,52], this may have influenced the initial phase of specific integrin interactions. The results of the contact angle measurements with ultrapure water on the experimental surfaces are summarized in supplementary material (table S1). The angles were about the same for pure glass and for glass coated with collagen or fibronectin. We therefore believe that wettability is not a predictor of MDFs in the early or late stages of cell adhesion.

4. Conclusion and outlook

The results of this study show, based on the example of two cell lines, that the cell adhesion forces develop significantly between the early stage and maturation. It is also shown that the MDFs in the initial and mature cell adhesion states have a different dependence on the substrate to which the cells adhere. Interestingly, the MDFs in the first adhesion phase are not a predictor for the MDFs in the mature phase, underlining the importance of quantifying both regimes of adhesion as a basis for the design of biointerfaces for a variety of applications. The initial adhesion processes may be a key factor for the successful colonization of the implant surfaces in the context of the "race to the surface", when prokaryotic microorganisms and somatic eukaryotic cells compete for adhesion to medical implant surfaces, as well as in the search for non-adhesive or cell-repellent surfaces e.g. for *in vivo* sensors and electrodes. Extending the analysis to the evolution of cell adhesion forces during maturation is of great interest in regenerative medicine as a tool for influencing and possibly directing cell proliferation and differentiation during healing processes and tissue formation.

Authors' statement

The manuscript includes contributions from all the authors. The authors have all approved the final version of the manuscript. None of the authors states any conflict of interest.

Funding sources

DFG (German Research Council), graduate school GRK1505/2"Welisa"

DFG (German Research Council), grant number BA 2479/2-1, "NeuroTRP"

ERC (European Research Council), grant number 617,989, “Design2Heal”

CRediT authorship contribution statement

Philipp Wysotzki: Conceptualization, Methodology, Software, Formal analysis, Investigation, Writing - original draft, Visualization. **Ana Sancho:** Conceptualization, Methodology, Investigation, Writing - original draft, Visualization. **Jan Gimsa:** Resources, Supervision, Writing - review & editing, Project administration, Funding acquisition, Writing - original draft. **Jürgen Groll:** Resources, Supervision, Writing - original draft, Project administration, Funding acquisition.

Declaration of Competing Interest

The authors declare that they have no known competing financial interests or personal relationships that could have appeared to influence the work reported in this paper.

Acknowledgments

The authors are grateful to the DFG (German Research Council) graduate school GRK1505/2 "Welisa" and grant number BA 2479/2-1 for funding the position of P. Wysotzki, as well as the consumables for the experiments. We also acknowledge the ERC (European Research Council), Grant Number 617989 for the financial support given. We are grateful to Dr. W. Baumann (Department of Biophysics, Univ. of Rostock) for helpful discussions.

Appendix A. Supplementary data

Supplementary material related to this article can be found, in the online version, at doi:https://doi.org/10.1016/j.colsurfb.2020.110894.

References

[1] M.L. Lastra, M.S. Molinuevo, I. Blaszczyk-Lezak, C. Mijangos, M.S. Cortizo, Nanostructured fumarate copolymer-chitosan crosslinked scaffold: an in vitro osteochondrogenesis regeneration study, *Journal of biomedical materials research*, Part A 106 (2018) 570–579, https://doi.org/10.1002/jbm.a.36260.

[2] J. Patterson, M.M. Martino, J.A. Hubbell, Biomimetic materials in tissue engineering, Mater. Today 13 (2010) 14–22, https://doi.org/10.1016/S1369-7021(10)70013-4.

[3] M.V. Beer, C. Rech, P. Gasteier, B. Sauerzapfe, J. Salber, A. Ewald, M. Möller, L. Elling, J. Groll, The next step in biomimetic material design: poly-LacNAc-mediated reversible exposure of extra cellular matrix components, Adv. Healthc. Mater. 2 (2013) 306–311, https://doi.org/10.1002/adhm.201200080.

[4] A. Rossi, L. Wistlich, K.-H. Heffels, H. Walles, J. Groll, Isotropic versus bipolar functionalized biomimetic artificial basement membranes and their evaluation in long-term human cell Co-culture, Adv. Healthc. Mater. 5 (2016) 1939–1948, https://doi.org/10.1002/adhm.201600224.

[5] L. Wistlich, J. Kums, A. Rossi, K.-H. Heffels, H. Wajant, J. Groll, Multimodal bioactivation of hydrophilic electrospun nanofibers enables simultaneous tuning of cell adhesivity and immunomodulatory effects, Adv. Funct. Mater. 27 (2017) 1702903, , https://doi.org/10.1002/adfm.201702903.

[6] A.A. Khalili, M.R. Ahmad, A. Khalili, M. Ahmad, A review of cell adhesion studies for biomedical and biological applications, Int. J. Mol. Sci. 16 (2015) 18149–18184, https://doi.org/10.3390/ijms160818149.

[7] S. Hong, E. Ergezen, R. Lec, K.A. Barbee, Real-time analysis of cell–surface adhesive interactions using thickness shear mode resonator, Biomaterials 27 (2006) 5813–5820, https://doi.org/10.1016/j.biomaterials.2006.07.031.

[8] H. Delanoe-Ayari, R. Al Kurdi, M. Vallade, D. Gulino-Debrac, D. Riveline, Membrane and acto-myosin tension promote clustering of adhesion proteins, Proc. Natl. Acad. Sci. 101 (2004) 2229–2234, https://doi.org/10.1073/pnas.0304297101.

[9] D. Riveline, E. Zamir, N.Q. Balaban, U.S. Schwarz, T. Ishizaki, S. Narumiya, Z. Kam, B. Geiger, A.D. Bershadsky, Focal contacts as mechanosensors: externally applied local mechanical force induces growth of focal contacts by an Mdia1-Dependent and rock-independent mechanism, J. Cell Biol. 153 (2001) 1175–1186.

[10] N. Strohmeyer, M. Bharadwaj, M. Costell, R. Fässler, D.J. Müller, Fibronectin-bound α5β1 integrins sense load and signal to reinforce adhesion in less than a second, Nat. Mater. 16 (2017) 1262–1270, https://doi.org/10.1038/nmat5023.

[11] A.J. García, P. Ducheyne, D. Boettiger, Quantification of cell adhesion using a spinning disc device and application to surface-reactive materials, Biomaterials 18 (1997) 1091–1098, https://doi.org/10.1016/S0142-9612(97)00042-2.

[12] J. Friedrichs, K.R. Legate, R. Schubert, M. Bharadwaj, C. Werner, D.J. Müller, M. Benoit, A practical guide to quantify cell adhesion using single-cell force spectroscopy, Methods 60 (2013) 169–178, https://doi.org/10.1016/j.ymeth.2013.01.006.

[13] C.A. Burdsal, M.M. Lotz, J. Miller, D.R. McClay, Quantitative switch in integrin expression accompanies differentiation of F9 cells treated with retinoic acid, Dev. Dyn. 201 (1994) 344–353, https://doi.org/10.1002/aja.1002010406.

[14] A.V. Taubenberger, D.W. Hutmacher, D.J. Muller, Single-cell force spectroscopy, an emerging tool to quantify cell adhesion to biomaterials, Tissue Eng. Part B Rev. 20 (2014) 40–55, https://doi.org/10.1089/ten.teb.2013.0125.

[15] G. Weder, O. Guillaume-Gentil, N. Matthey, F. Montagne, H. Heinzelmann, J. Vörös, M. Liley, The quantification of single cell adhesion on functionalized surfaces for cell sheet engineering, Biomaterials 31 (2010) 6436–6443, https://doi.org/10.1016/j.biomaterials.2010.04.068.

[16] E. Potthoff, O. Guillaume-Gentil, D. Ossola, J. Polesel-Maris, S. LeibundGut-Landmann, T. Zambelli, J.A. Vorholt, Rapid and serial quantification of adhesion forces of yeast and mammalian cells, PLoS One 7 (2012) e52712, , https://doi.org/10.1371/journal.pone.0052712.

[17] A. Meister, M. Gabi, P. Behr, P. Studer, J. Vörös, P. Niedermann, J. Bitterli, J. Polesel-Maris, M. Liley, H. Heinzelmann, T. Zambelli, Fluid FM: combining atomic force microscopy and nanofluidics in a universal liquid delivery system for single cell applications and beyond, Nano Lett. 9 (2009) 2501–2507, https://doi.org/10.1021/nl901384x.

[18] E. Potthoff, D. Franco, V. D'Alessandro, C. Starck, V. Falk, T. Zambelli, J.A. Vorholt, D. Poulikakos, A. Ferrari, Toward a rational design of surface textures promoting endothelialization, Nano Lett. 14 (2014) 1069–1079, https://doi.org/10.1021/nl4047398.

[19] A. Sancho, I. Vandersmissen, S. Craps, A. Luttun, J. Groll, A new strategy to measure intercellular adhesion forces in mature cell-cell contacts, Sci. Rep. 7 (2017) 46152, https://doi.org/10.1038/srep46152.

[20] R. Zange, T. Kissel, Comparative in vitro biocompatibility testing of poly-cyanoacrylates and poly(d,l-lactide-co-glycolide) using different mouse fibroblast (L929) biocompatibility test models, Eur. J. Pharm. Biopharm. 44 (1997) 149–157, https://doi.org/10.1016/S0939-6411(97)00082-9.

[21] A.G. Karakecili, T.T. Demirtas, C. Satriano, M. Gümüsderelioglu, G. Marletta, Evaluation of L929 fibroblast attachment and proliferation on Arg-Gly-Asp-Ser (RGDS)-immobilized chitosan in serum-containing/serum-free cultures, J. Biosci. Bioeng. 104 (2007) 69–77, https://doi.org/10.1263/jbb.104.69.

[22] M. Maldonado, J. Nam, The role of changes in extracellular matrix of cartilage in the presence of inflammation on the pathology of osteoarthritis, Biomed Res. Int. 2013 (2013) 284873, https://doi.org/10.1155/2013/284873.

[23] Y. Takeuchi, M. Suzawa, T. Kikuchi, E. Nishida, T. Fujita, T. Matsumoto, Differentiation and transforming growth Factor-β receptor down-regulation by Collagen-α2β1 integrin interaction is mediated by focal adhesion kinase and its downstream signals in murine osteoblastic cells, J. Biol. Chem. 272 (1997) 29309–29316, https://doi.org/10.1074/jbc.272.46.29309.

[24] H. Sudo, In vitro differentiation and calcification in a new clonal osteogenic cell line derived from newborn mouse calvaria, J. Cell Biol. 96 (1983) 191–198, https://doi.org/10.1083/jcb.96.1.191.

[25] S. Bonk, P. Oldorf, R. Peters, W. Baumann, J. Gimsa, Fast prototyping of sensorized cell culture chips and microfluidic systems with ultrashort laser pulses, Micromachines 6 (2015) 364–374, https://doi.org/10.3390/mi6030364.

[26] P. Wysotzki, J. Gimsa, Surface coatings modulate the differences in the adhesion forces of eukaryotic and prokaryotic cells as detected by single cell force microscopy, Int. J. Biomater. 2019 (2019) 1–12, https://doi.org/10.1155/2019/7024259.

[27] L. Jia, F. Han, H. Wang, C. Zhu, Q. Guo, J. Li, Z. Zhao, Q. Zhang, X. Zhu, B. Li, Polydopamine-assisted surface modification for orthopaedic implants, J. Orthop. Translat. 17 (2019) 82–95, https://doi.org/10.1016/j.jot.2019.04.001.

[28] J.H. Ryu, P.B. Messersmith, H. Lee, Polydopamine surface chemistry: a decade of discovery, ACS Appl. Mater. Interfaces 10 (2018) 7523–7540, https://doi.org/10.1021/acsami.7b19865.

[29] Z. Wang, H.-C. Yang, F. He, S. Peng, Y. Li, L. Shao, S.B. Darling, Mussel-inspired surface engineering for water-remediation materials, Matter 1 (2019) 115–155, https://doi.org/10.1016/j.matt.2019.05.002.

[30] H. Lee, S.M. Dellatore, W.M. Miller, P.B. Messersmith, Mussel-inspired surface chemistry for multifunctional coatings, Science 318 (2007) 426–430, https://doi.org/10.1126/science.1147241.

[31] Q. Ye, F. Zhou, W. Liu, Bioinspired catecholic chemistry for surface modification, Chem. Soc. Rev. 40 (2011) 4244–4258, https://doi.org/10.1039/c1cs15026j.

[32] J.L. Hutter, J. Bechhoefer, Calibration of atomic-force microscope tips, Rev. Sci. Instrum. 64 (1993) 1868–1873, https://doi.org/10.1063/1.1143970.

[33] M. Shamir, Y. Bar-On, R. Phillips, R. Milo, SnapShot: timescales in cell biology, 1302-1302.e1, Cell 164 (2016), https://doi.org/10.1016/j.cell.2016.02.058.

[34] C. Selhuber-Unkel, T. Erdmann, M. López-García, H. Kessler, U.S. Schwarz, J.P. Spatz, Cell adhesion strength is controlled by intermolecular spacing of adhesion receptors, Biophys. J. 98 (2010) 543–551, https://doi.org/10.1016/j.bpj.2009.11.001.

[35] E. Gladilin, A. Micoulet, B. Hosseini, K. Rohr, J. Spatz, R. Eils, 3D finite element analysis of uniaxial cell stretching: from image to insight, Phys. Biol. 4 (2007) 104–113, https://doi.org/10.1088/1478-3975/4/2/004.

[36] G.E. Jones, Fibronectin glycosylation modulates fibroblast adhesion and spreading, J. Cell Biol. 103 (1986) 1663–1670, https://doi.org/10.1083/jcb.103.5.1663.

[37] A.-M. Galow, A. Rebl, D. Koczan, S.M. Bonk, W. Baumann, J. Gimsa, Increased osteoblast viability at alkaline pH in vitro provides a new perspective on bone regeneration, Biochem. Biophys. Rep. 10 (2017) 17–25, https://doi.org/10.1016/j.

bbrep.2017.02.001.
[38] P.W. Hwang, J.A. Horton, Variable osteogenic performance of MC3T3-E1 subclones impacts their utility as models of osteoblast biology, Sci. Rep. 9 (2019) 8299, https://doi.org/10.1038/s41598-019-44575-8.
[39] R.T. Franceschi, B.S. Iyer, Y. Cui, Effects of ascorbic acid on collagen matrix formation and osteoblast differentiation in murine MC3T3-E1 cells, J. Bone Miner. Res. 9 (1994) 843–854, https://doi.org/10.1002/jbmr.5650090610.
[40] A.D. Bershadsky, N.Q. Balaban, B. Geiger, Adhesion-dependent cell mechanosensitivity, Annu. Rev. Cell Dev. Biol. 19 (2003) 677–695, https://doi.org/10.1146/annurev.cellbio.19.111301.153011.
[41] A. Engler, L. Bacakova, C. Newman, A. Hategan, M. Griffin, D. Discher, Substrate compliance versus ligand density in cell on gel responses, Biophys. J. 86 (2004) 617–628, https://doi.org/10.1016/S0006-3495(04)74140-5.
[42] J. Xie, M. Bao, S.M.C. Bruekers, W.T.S. Huck, Collagen gels with different fibrillar microarchitectures elicit different cellular responses, ACS Appl. Mater. Interfaces 9 (2017) 19630–19637, https://doi.org/10.1021/acsami.7b03883.
[43] R.J. Pelham, Y.-l. Wang, Cell locomotion and focal adhesions are regulated by substrate flexibility, Proc Natl Acad Sci U S A 94 (1997) 13661–13665.
[44] P.C. Georges, P.A. Janmey, Cell type-specific response to growth on soft materials, J. Appl. Physiol. 2005 (98) (1985) 1547–1553, https://doi.org/10.1152/japplphysiol.01121.2004 (Bethesda, Md..
[45] D.E. Discher, P. Janmey, Y.-l. Wang, Tissue cells feel and respond to the stiffness of their substrate, Science 310 (2005) 1139–1143, https://doi.org/10.1126/science.1116995.
[46] N.C. Gauthier, T.A. Masters, M.P. Sheetz, Mechanical feedback between membrane tension and dynamics, Trends Cell Biol. 22 (2012) 527–535, https://doi.org/10.1016/j.tcb.2012.07.005.
[47] G.I. Bell, M. Dembo, P. Bongrand, Cell adhesion. Competition between nonspecific repulsion and specific bonding, Biophys. J. 45 (1984) 1051–1064, https://doi.org/10.1016/S0006-3495(84)84252-6.
[48] S.P. Carey, J.M. Charest, C.A. Reinhart-King, A. Gefen (Ed.), Cellular and Biomolecular Mechanics and Mechanobiology, Springer, Berlin, Heidelberg, New York, 2011, pp. 29–69.
[49] J.T. Parsons, A.R. Horwitz, M.A. Schwartz, Cell adhesion: integrating cytoskeletal dynamics and cellular tension, Nat. Rev. Mol. Cell Biol. 11 (2010) 633–643, https://doi.org/10.1038/nrm2957.
[50] T. Hoshiba, C. Yoshikawa, K. Sakakibara, Characterization of initial cell adhesion on charged polymer substrates in serum-containing and serum-free media, Langmuir 34 (2018) 4043–4051, https://doi.org/10.1021/acs.langmuir.8b00233.
[51] A.M. Nunes, C.A.S.A. Minetti, D.P. Remeta, J. Baum, Magnesium activates microsecond dynamics to regulate integrin-collagen recognition, Structure 2018 (26) (1993) 1080–1090.e5, https://doi.org/10.1016/j.str.2018.05.010 *(London*, England.
[52] S. Tiwari, J.A. Askari, M.J. Humphries, N.J. Bulleid, Divalent cations regulate the folding and activation status of integrins during their intracellular trafficking, J. Cell. Sci. 124 (2011) 1672–1680, https://doi.org/10.1242/jcs.084483.